Quantitative Biology 2021, 9(3): 329–340
https://doi.org/10.15302/J-QB-021-0237

RESEARCH ARTICLE

Systems analysis of the "weights" of Bcl-2 and Mcl-1 in mitochondrial apoptosis pathway establishes a predictor for best drug combination ratio

Zongwei Guo[1], Fangkui Yin[2], Peiran Wang[2], Ting Song[2,*], Zhichao Zhang[2,*]

[1] School of Bioengineering, Dalian University of Technology, Dalian 116024, China
[2] State Key Laboratory of Fine Chemicals, School of Chemistry, Dalian University of Technology, Dalian 116024, China
* Correspondence: songting@dlut.edu.cn, zczhang@dlut.edu.cn

Received June 22, 2020; Revised September 13, 2020; Accepted September 30, 2020

***Background*: Inhibitors of B-cell CLL/lymphoma 2 (Bcl-2) family proteins have shown hope as antitumor drugs. While the notion that it is efficient to coordinate, balance, and neutralize both arms of the anti-apoptotic Bcl-2 family has been validated in many cancer cells, the weights of the two arms contributing to apoptosis inhibition have not been explored. This study analyzed the best combination ratio for different Bcl-2 selective inhibitors.**

***Methods*: We used a previously established mathematical model to study the weights of Bcl-2 (representing both Bcl-2 and Bcl-xL in this study) and myeloid cell leukemia-1 (Mcl-1). Correlation and single-parameter sensitivity analysis were used to find the major molecular determinants for Bcl-2 and Mcl-1 dependency, as well as their weights. Biological experiments were used to verify the mathematical model.**

***Results*: Bcl-2 protein level and Mcl-1 protein level, production, and degradation rates were the major molecular determinants for Bcl-2 and Mcl-1 dependency. The model gained agreement with the experimental assays for ABT-737/A-1210477 and ABT-737/compound 5 combination effect in MCF-7 and MDA-MB-231. Two sets of equations composed of Bcl-2 and Mcl-1 levels were obtained to predict the best combination ratio for Bcl-2 inhibitors with Mcl-1 inhibitors that stabilize and downregulate Mcl-1, respectively.**

***Conclusions*: The two sets of equations can be used as tools to bypass time-consuming and laborious experimental screening to predict the best drug combination ratio for treatment.**

Keywords: weights of Bcl-2/Mcl-1; drug-target network; Bcl-2/Mcl-1 inhibitors combination; mathematical modeling

Author summary: We used a mathematical model combined with experimental verification to quantitatively examine the contribution of the two arms of anti-apoptotic Bcl-2 proteins to apoptosis by weight. The correlation analysis and single-parameter sensitivity analysis showed that Bcl-2 protein level and Mcl-1 protein level, production, and degradation rates were the major molecular determinants. We gained two sets of equations as tools to bypass the time-consuming and laborious experimental screening to predict the best drug combination ratio for treatment. Biological experiments have verified the efficiency of the tools in MCF-7, MDA-MB-231, OCI-AML3, and HCT-116 cells.

INTRODUCTION

The intrinsic apoptosis process is tightly regulated by the B-cell CLL/lymphoma 2 (Bcl-2) family of proteins [1,2]. Based on their Bcl-2 homology (BH) domains, Bcl-2 proteins can be grouped into three subfamilies: the anti-apoptotic Bcl-2-like member, the pro-apoptotic Bax-like member, and the pro-apoptotic BH3-only protein member

[3]. Cancer cells often aberrantly overexpress anti-apoptotic Bcl-2 family proteins to protect cells, which are primed for apoptosis [4,5]. Therefore, Bcl-2 inhibitors are promising anti-tumor agents that neutralize anti-apoptotic Bcl-2-like proteins by binding to the BH3 groove, leading to Bax and Bak oligomerize in the mitochondrial outer membrane to form pores that release apoptotic proteins into the cytosol and trigger a downstream cascade of apoptosis [6,7]. The anti-apoptotic members counteract the pro-apoptotic members via a shared BH3 domain, and the multi-interplay between anti-apoptotic Bcl-2-like members and Bcl-2 inhibitors constitute a drug-target network which can estimate drug effect on target perturbations in the whole system [8].

Anti-apoptotic Bcl-2 family members can be divided into two groups, one mainly comprising Bcl-2 and Bcl-2-like protein 1 isoform 1 (Bcl-xL), and the other mainly containing myeloid cell leukemia-1 (Mcl-1). Efficient apoptosis and effective therapy have been shown to require coordinated neutralization of both arms of anti-apoptotic proteins [9–12]. For example, ABT-737 is a subnanomolar inhibitor of Bcl-2 and Bcl-xL [13,14]. Although ABT-737 induces potent apoptosis in cancer cell lines derived from small-cell lung carcinomas (SCLC) and B-cell lymphomas, the majority of cell lines derived from other tumors showed resistance to ABT-737 as monotherapy, whereas combination of ABT-737 with Mcl-1 siRNA or Mcl-1 specific inhibitors could efficiently induce apoptosis in these cell lines [15–18]. Because the two arms of anti-apoptotic Bcl-2 proteins cooperate to inhibit apoptosis in the disease network, combination of Bcl-2 and Mcl-1 inhibitors can act on the two targets in the network at the same time, and have a synergistic effect on each target [19,20]. If the two targets are attacked simultaneously in a coordinated and balanced ratio, the total effect achieved could be greater than treatment with one or the other, having the best therapeutic effect [21,22]. However, no studies have quantitatively examined the contribution of the two arms of anti-apoptotic Bcl-2 proteins to apoptosis, that is the weights of Bcl-2/Bcl-xL and Mcl-1, which is directly related to the best combination ratio.

A well-established network model using ordinary differential equations (ODEs) and mathematical simulations via Bcl-2 multi-protein interaction interplay has been successfully used to obtain a quantitative and kinetic understanding of the apoptosis regulation. For example, Prehn *et al.* established and used mathematical model of Bcl-2 interactions (DR_MOMP) to predict responses to chemotherapy in colorectal cancer [23], identify high-risk colorectal cancer patients [24] and accurately predict responses to genotoxic agents and their synergism with Bcl-2 inhibitors in triple negative breast cancer cells [25]. Rehm *et al.* used a combined approach of deterministic mathematical modeling and experimental validation to reveal that Bax retro-translocation potentiates Bcl-xL's anti-apoptotic activity [26]. However, these models did not explore the weights of anti-apoptotic Bcl-2 proteins and predict best combination ratio.

Mcl-1 differs from the other arm of Bcl-2 family (Bcl-2/Bcl-xL) in having a very short half-life [27,28]. In addition, quick upregulation or downregulation of Mcl-1 level often occurs during apoptosis [29]. Although many predictions utilized a multi-protein index to predict Mcl-1 dependency, for example, the ratio of Mcl-1 to Bcl-xL to predict Mcl-1 dependency in none small-cell lung carcinomas (NSCLC) [30], lack of consideration for Mcl-1 dynamics in addition to static Mcl-1 levels would influence the accuracy of the prediction. Importantly, some Mcl-1 inhibitors have been found that inhibits and facilitates Mcl-1 degradation in an opposite way, as exemplified by A-1210477 [31] and compound 5 [32], respectively.

Herein, we used the ODEs model to study the weights of Bcl-2 (represent both Bcl-2 and Bcl-xL thereafter) and Mcl-1. After validating model predictions with experimental findings, the model has revealed that Bcl-2 expression level, Mcl-1 expression level, Mcl-1 production and degradation rate constitute the molecular determinants for Bcl-2 and Mcl-1 dependency. Two equations were established that could predict the best combination ratio for Bcl-2 and Mcl-1 inhibitors that stabilize and de-stabilize Mcl-1, respectively. The equations were further validated in the MCF-7, MDA-MB-231, OCI-AML3, and HCT-116 cell lines.

RESULTS

A systematic model to quantitatively analyze the different concentrations of Bcl-2 and Mcl-1 in apoptosis signaling

Bcl-2 and Mcl-1 proteins have very different protein stabilities (20-fold differences in half-life time) and individual antagonistic effects on apoptosis in tumor cells. Therefore, the proportional inhibitory effects of the two proteins have different contributions to mitochondrial outer membrane permeabilization (MOMP). It indicated that Bcl-2 and Mcl-1 would have different weights in inhibiting MOMP, but the values remained unclear (Fig. 1, the edge weight of Bcl-2 and Mcl-1 is labeled in gray).

To quantitatively analyze the different weights of anti-apoptotic Bcl-2 family proteins in the process of MOMP, we performed a mathematical model using ODEs (Supplementary Tables S1–S6). The proteins with similar biochemical reactions were presented by single kinds in

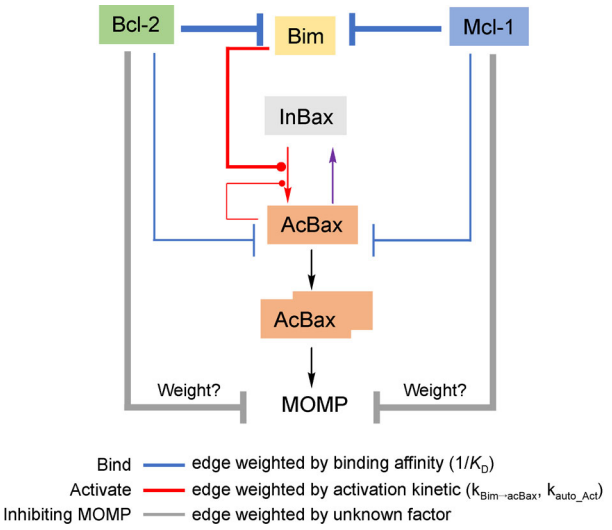

Figure 1. Mathematical model of Bcl-2-controlled MOMP that was formulated in terms of Bcl-2 protein interactions. The red line indicated Bax activation by Bim or auto-activation. The blue line indicated Bcl-2 and Mcl-1 binding with pro-apoptotic Bim and activated Bax. The dimerization of Bax indicated by black line served as the model output. The individual contribution of Bcl-2 and Mcl-1 to block MOMP (weights of Bcl-2 and Mcl-1) remains to be determined. (AcBax is the abbreviation of Activated Bax, InBax is the abbreviation of Inactivated Bax)

our model. Such as both Bax represents effector Bcl-2 proteins (both Bax and Bak). Bim represents activator BH3-only proteins (Bim and Puma). Bcl-2 represents both Bcl-2 and Bcl-xL [33]. Given the very different protein half-life of Mcl-1 compared to Bcl-2, Mcl-1 serves as independent species. Among the six anti-apoptotic Bcl-2 family members, Bcl-2, Bcl-xL and Mcl-1 are the most abundantly expressed ones in cancer cells [34], and thus they are modeled to serve as the major guards for MOMP. It is a well-built approach based on the widely admitted topological properties of the Bcl-2-family protein interaction network (Fig. 1). The induction of MOMP occurred by inhibition of Bcl-2 and/or Mcl-1 that leads to activator BH3-only proteins Bim to activate effector Bax, resulting in their homo-oligomerization. MOMP was assumed to occur when more than 10% of total effectors form oligomers [23].

Using the simplified model of the mitochondrial apoptosis pathways, we quested for quantifying the concentrations of Bcl-2 and Mcl-1 in different cancer cell lines. In the following section, we used knockdown of Bcl-2 and/or Mcl-1 as the input signal, which was experimentally resembled by inhibitor treatment. Subsequently, we calculated the amounts of Bax oligomers under a given input by solving ODEs, based on which whether MOMP occurs could be predicted.

Systematic modeling resembles experimental findings of various dependencies or co-dependencies of different kinds of cancer on Bcl-2 and Mcl-1

The different weights of Bcl-2 and Mcl-1 in the tumor molecular network led to different dependences on Bcl-2 and Mcl-1 of tumor cells. To investigate whether the model is suitable to identify the weights of Bcl-2 and Mcl-1 for MOMP inhibition, it was required to verify whether the model calculation results were accordant with the experimental findings on Bcl-2 and/or Mcl-1 dependency in a panel of cancer cell lines.

Firstly, we chose a panel of 30 cell lines (Table 1) which have been reviewed to be dependent on single Bcl-2, Mcl-1 or combination of the two proteins [35], and then verified the recovery of expected dependencies by modeling. The expression levels of Bcl-2 family proteins in the cell line panel were determined as shown in Materials and methods, and then parameterized in the model (Table 1). The production rate of single Bcl-2 (parameter kpro_Bcl-2 in model, see Supplementary Table S1) which was input with 0 in the model resembles the experimental cell line treatment by specific Bcl-2 inhibitor; The production rate of single Mcl-1 (parameter kpro_Mcl-1 in model, see Supplementary Table S1) which was input with 0 in the model resembles the experimental cell line treatment by specific Mcl-1 inhibitor; Both of the production rates (kpro_Bcl-2 and kpro_Mcl-1) which were input with 0 simultaneously in the model resembles the experimental cell line treatment by specific Bcl-2 and Mcl-1 inhibitor in combination. Based on that, the amounts of oligomers were calculated to test MOMP occurrence in the above three cases for the panel of cell lines, respectively. If abrogating either of Bcl-2 and Mcl-1 could induce MOMP, the cell line is predicted as single Bcl-2 dependency and Mcl-1 dependency, respectively (shown with circle and triangle in Table 1, the second column). If MOMP does not occur only when both Bcl-2 and Mcl-1 are absent, the cell line is predicted as Bcl-2 + Mcl-1 co-dependency (shown with square in Table 1, the second column).

Then, we compared the model prediction with the experimental findings (Table 1, the third column). An agreement between model prediction and the experimental findings was gained in 27 of the 30 cell lines.

Following this, we sought to confirm the decisive molecular factors of the significant responses in the cell line profiles various dependencies on Bcl-2 and Mcl-1. The 27 cell lines with some type of Bcl-2 dependency were grouped based on their dependencies: 1. single or co-dependency on Bcl-2 versus non-dependency on Bcl-2; 2. single or co-dependency on Mcl-1 versus non-dependency on Mcl-1. As shown in Fig. 2A, the expression level of Bcl-2 discriminates the group with

Table 1 Model predicted Bcl-2 and/or Mcl-1 dependency in comparison with experimental finding in literature

Cell lines (30)	Model prediced dependency	Experimentally determined dependency	Bcl-2 level (nM)	Bcl-xL level (nM)	Mcl-1 level (nM)	Bax level (nM)	Bak level (nM)	Puma level (nM)	Bim level (nM)
RS4;11	●	●	280	300	35	312	224	8	8
MOLM-13	●	●	351	289	42	276	285	13	6
MDA-MB-231[a]	●	●	225	145	125	332	301	7	11
NCI-H23	▲	▲	14	20	145	236	520	9	15
MCF-7[a]	▲	▲	283	163	188	270	314	13	9
OCI-AML3[b]	▲	▲	213	104	226	294	280	16	7
T-47D	■	■	312	112	102	341	330	19	6
HCT-116[a]	■	■	247	576	31	327	655	21	13
THP-1[a]	■	■	186	98	72	286	320	18	12
Hep-G2	■	■	340	354	82	254	231	11	17
SNU-423	●	●	379	127	55	432	176	7	9
Panc 10.05	●	●	402	252	58	358	417	15	10
U-118MG	●	●	174	388	94	258	479	16	22
AU-565	▲	▲	24	20	93	425	328	12	13
HCC-1954	▲	▲	41	32	105	267	422	8	19
SK-BR-3	▲	▲	45	21	89	350	346	20	8
BT-20	▲	▲	53	45	112	278	531	15	9
Capan-1	▲	▲	62	25	95	356	321	10	16
COLO-679	■	▲	368	184	105	402	255	9	12
HCC-1395	■	▲	319	305	87	268	521	14	18
CFPAC-1	▲	▲	46	36	107	325	379	11	15
DBTRG-05MG	■	●	287	228	85	246	321	13	7
SK-MEL-5	●	●	314	191	64	332	412	15	11
SK-MEL-28	●	●	520	115	101	542	164	18	16
OV-90	■	■	311	269	120	348	317	14	12
Panc 02.03	■	■	276	264	92	259	415	10	13
SW-480	●	●	458	217	83	452	316	8	14
Hs-766T	■	■	546	364	128	387	464	9	11
SW-948	■	■	241	332	102	259	523	14	10
A-172	■	■	641	211	130	521	357	16	9

●Bcl-2 dependency ▲ Mcl-1 dependency ■ Bcl-2 + Mcl-1 co-dependency

[a] The protein levels have been experimentally determined in our previous study [46].

[b] The protein levels have been experimentally determined in our previous study [47].

Bcl-2 dependency from the Bcl-2 non-dependency group ($P < 0.001$), indicating that there was a significant positive correlation between the expression level of Bcl-2 and Bcl-2 dependence across cell lines.

The expression level of Mcl-1 exhibited significant while moderate differences between the Mcl-1 dependency and Mcl-1 non-dependency groups ($P < 0.05$) (Fig. 2B). In addition, the production rate of Mcl-1 displayed a significantly strong difference ($P < 0.001$) (Fig. 2C).

Indeed, the ratio of Bcl-2 turnover ($k_{pro\_Bcl\text{-}2}$ /$k_{deg\_Bcl\text{-}2}$, Supplementary Tables S1 and S4) was also correlated with Bcl-2 dependency because the level of the long-lived protein was proportional to its dynamics. In contrast, for the short-lived Mcl-1, there was a separation between the static equilibrium levels of Mcl-1 with the ratio of its turnover ($k_{pro\_Mcl\text{-}1}$ /$k_{deg\_Mcl\text{-}1}$, Supplementary Tables S1 and S4). Importantly, our modeling results showed that the production rate of Mcl-1 also plays a significant role in Mcl-1 dependency.

Taken together, the model accurately predicted the experimental findings on Bcl-2 and/or Mcl-1 dependency, indicating the applicability of the model to study the weights of Bcl-2 and Mcl-1. Moreover, the verified model showed that the static level of Bcl-2 could predict single or co-dependency on Bcl-2. However, the static levels of

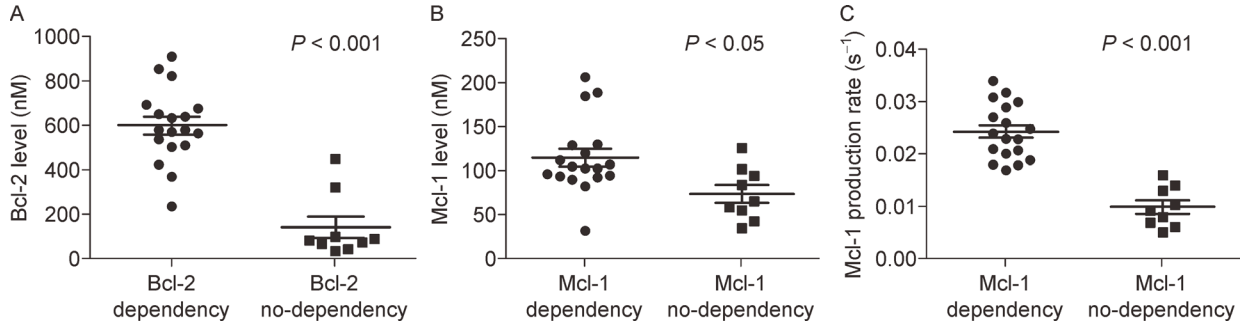

Figure 2. Correlation analysis of Bcl-2 protein levels, Mcl-1 protein levels, and Mcl-1 production rates with Bcl-2 or Mcl-1 dependency. (A) Grouping cell lines by dependency versus non-dependency on Bcl-2 was correlated to Bcl-2 levels. (B, C) Grouping cell lines by dependency versus non-dependency on Mcl-1 was correlated to Mcl-1 levels and Mcl-1 production rates, respectively.

Mcl-1 had a less predictive value because the Mcl-1 production rate was another influencing factor.

Model predicted different weights of Bcl-2 and Mcl-1 by controlling drug ratios

If Bcl-2 and Mcl-1 have different weights that contribute to MOMP inhibition in the apoptosis network, a balanced drug ratio (λ) to target Bcl-2 and Mcl-1 will exist, leading to the best synergistic effect. For quantitative analysis of the weights of Bcl-2 and Mcl-1, we modeled amounts of Bax oligomers in response to a specific Bcl-2 and Mcl-1 inhibitors alone or in combination under a prescribed set of fixed ratios (the dose of one drug is escalated while the dose of the other one remains constant), which was varied in a wide range. Different dose-ratios can be compared using the combination index (CI) values as in our previous study [36].

To date, several specific Bcl-2 inhibitors and Mcl-1 inhibitors have been reported. Their binding affinities have been experimentally determined and could be parameterized in the model to express the chemical inhibition of Bcl-2 and Mcl-1 alone or in combination. Here, we used ABT-737 as an example of a Bcl-2 inhibitor, and the parameter was derived from the literature [37]. ABT-737 is a dual Bcl-2/Bcl-xL inhibitor and served as a specific Bcl-2 inhibitor and represents both Bcl-2 and Bcl-xL in our model. For Mcl-1, A-1210477 and compound 5 were used as inhibitors [31,32]. Mcl-1 is a short-lived protein, and binding in its BH3 groove influences its stability. A-1210477 is an Mcl-1 inhibitor that inhibits Mcl-1 degradation through competitive binding with Mule [31]. Consistently, we detected dose-dependent Mcl-1 upregulation upon treatment with A-1210477 (Fig. 3A, top panel). In contrast, compound 5, previously developed in our lab [32], is a dual-function inhibitor that targets the Mcl-1 BH3 domain and induces Mcl-1 degradation by facilitating Mule binding (Fig. 3B, top panel). The effect of A-1210477 and compound 5 on influencing Mcl-1 degradation rate is described by equations in Supplementary Table S4. The parameters were fitted to the experimental data of changes in Mcl-1 levels upon A-1210477 or compound 5 treatments (Fig. 3A and B, bottom panel).

Then, we modeled the ability of the combination of ABT-737 with A-1210477 or compound 5 to induce MOMP in a panel of 10 cancer cell lines (RS4; 11, MOLM-13, MDA-MB-231, NCI-H23, MCF-7, OCI-AML3, T47-D, HCT-116, THP-1, and Hep-G2) with a fixed ratio varying from 32:1 to 1:32. The degree of synergism (CI value) was calculated.

By modeling, we found the best drug ratio λ to produce the lowest CI value predicted for the inhibitor combinations among the 10 cell lines. As shown in Fig. 4A and B, for ABT-737/A-1210477, the best drug ratio λ was 1:1 for RS4;11, MOLM-13, NCI-H23, MCF-7, T47-D, and THP-1. It was 2:1 for HCT-116 and Hep-G2, and 1:2 for MDA-MB-231 and OCI-AML3. For ABT-737/ compound 5, the best drug ratio λ was 1:1 for RS4;11, MOLM-13, NCI-H23, OCI-AML3, T47-D, and THP-1. It was 2:1 for MCF-7, HCT-116, and Hep-G2, and 1:2 for MDA-MB-231.

To test whether the model predicted combination ratio could recapitulate the synergy experiments with the Bcl-2 and Mcl-1 inhibitor combinations under different drug ratios, we selected MCF-7 and MDA-MB-231 to perform the drug combination experiment. An Annexin V-FITC Apoptosis assay determined the experimental LC_{50} value after 48 h of exposure to the compounds. The CI values were calculated using parameters obtained from the median-effect plots of ABT-737 alone, A-1210477 alone, compound 5 alone, and combinations of ABT-737/A-1210477 or ABT-737/compound 5 at fixed ratios ranging from 1:4 to 4:1. As shown in Fig. 5A and B, a broad spectrum of CI values ranging from 0.39 to 0.96 were determined for MCF-7. The lowest CI value was observed with a drug ratio of 1:1 for ABT-737/A-1210477 (CI = 0.39, $P < 0.01$), whereas it was 2:1 for

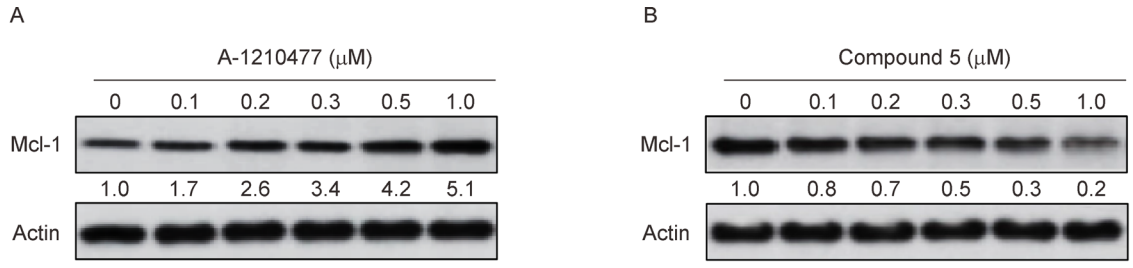

Parameter statistics	Best	Min	Max	Mean	Quantiles 5%	Quantiles 95%	Units
$k_{deg\_Mcl/A1210477}$	8.52E−05	7.84E−05	8.92E−05	8.41E−05	8.22E−05	8.76E−05	s^{-1}
$k_{deg\_Mcl/com\ 5}$	4.14E−04	3.96E−04	4.53E−04	4.02E−04	4.08E−04	4.48E−04	s^{-1}

Figure 3. Statistical analysis of the best-fit parameter for the degradation rates of Mcl-1/A-1210477 and Mcl-1/compound 5. (A, B) MCF-7 cells were treated with increasing concentrations of A-1210477 (A) or compound 5 (B) for 24 h, the Mcl-1 level was determined by immunoblotting. Data are the mean±stand deviation (sd) ($n = 3$). The optimal parameter sets were found using the MATLAB Optimization toolbox to minimize the error between the data and model simulations.

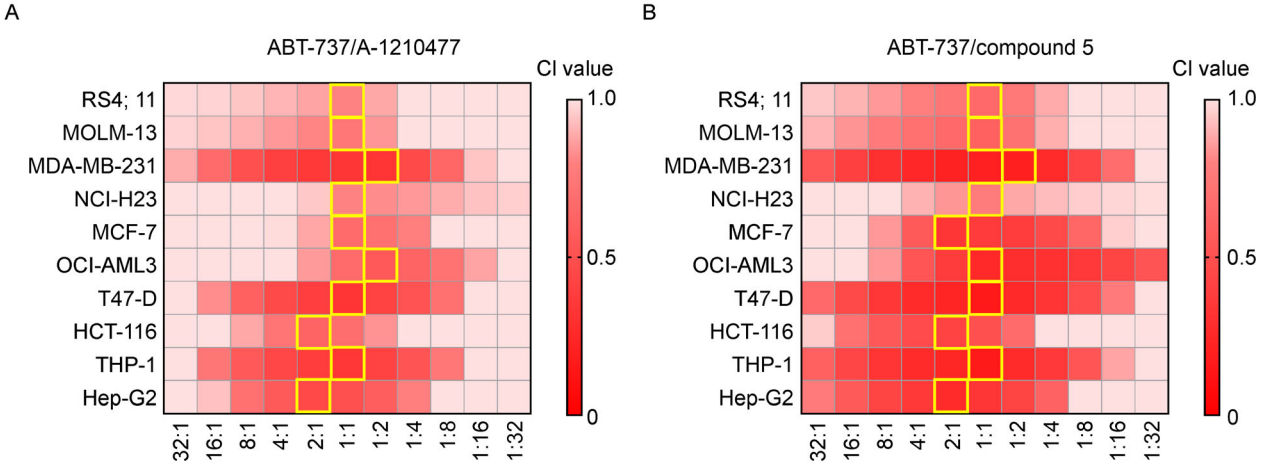

Figure 4. The model predicted best combination ratios of ABT-737/A-1210477 and ABT-737/compound 5 in various cancers. (A, B) The model predicted dose of ABT-737, A-1210477, and compound 5 alone or in combination at a range of fixed ratios for MOMP was used to calculate the CI value, wherein the lowest CI value was highlighted in yellow.

ABT-737/ compound 5 (CI = 0.42, $P < 0.01$). For MDA-MB-231, CI values ranged from 0.25 to 0.83. The lowest CI value was observed with a drug ratio of 1:2 for both ABT-737/A-1210477 (CI = 0.25, $P < 0.01$) and ABT-737/ compound 5 (CI = 0.31, $P < 0.01$) (Fig. 5C and D). The experimental results were consistent with the model predictions in MCF-7 and MDA-MB-231 cells.

To identify which parameters had a major impact on the weights of Bcl-2 and Mcl-1 in our model, we performed a single-parameter sensitivity analysis to identify the best drug ratio λ by increasing or decreasing the equilibrium levels of Bcl-2, Mcl-1, Bax, Bim, and other parameters by 5%. Then we recorded the percentage change of the best drug ratio λ. As shown in Fig. 6, the levels of Bcl-2 and Mcl-1, as well as the degradation rate of Mcl-1/inhibitors, led to a λ shift greater than 3%, indicating that the weights of Bcl-2 and Mcl-1 influence optimal inhibitor activation. The levels of Bax and Bim, as well as other parameters, led to a λ shift of less than 1%, indicating that they have little influence on the weights of Bcl-2 and Mcl-1.

Combined with experimental validation, the model study revealed that the weights of Bcl-2 and Mcl-1 mainly depend on Bcl-2 and Mcl-1 levels and the Mcl-1 production and degradation rates, as similar in their

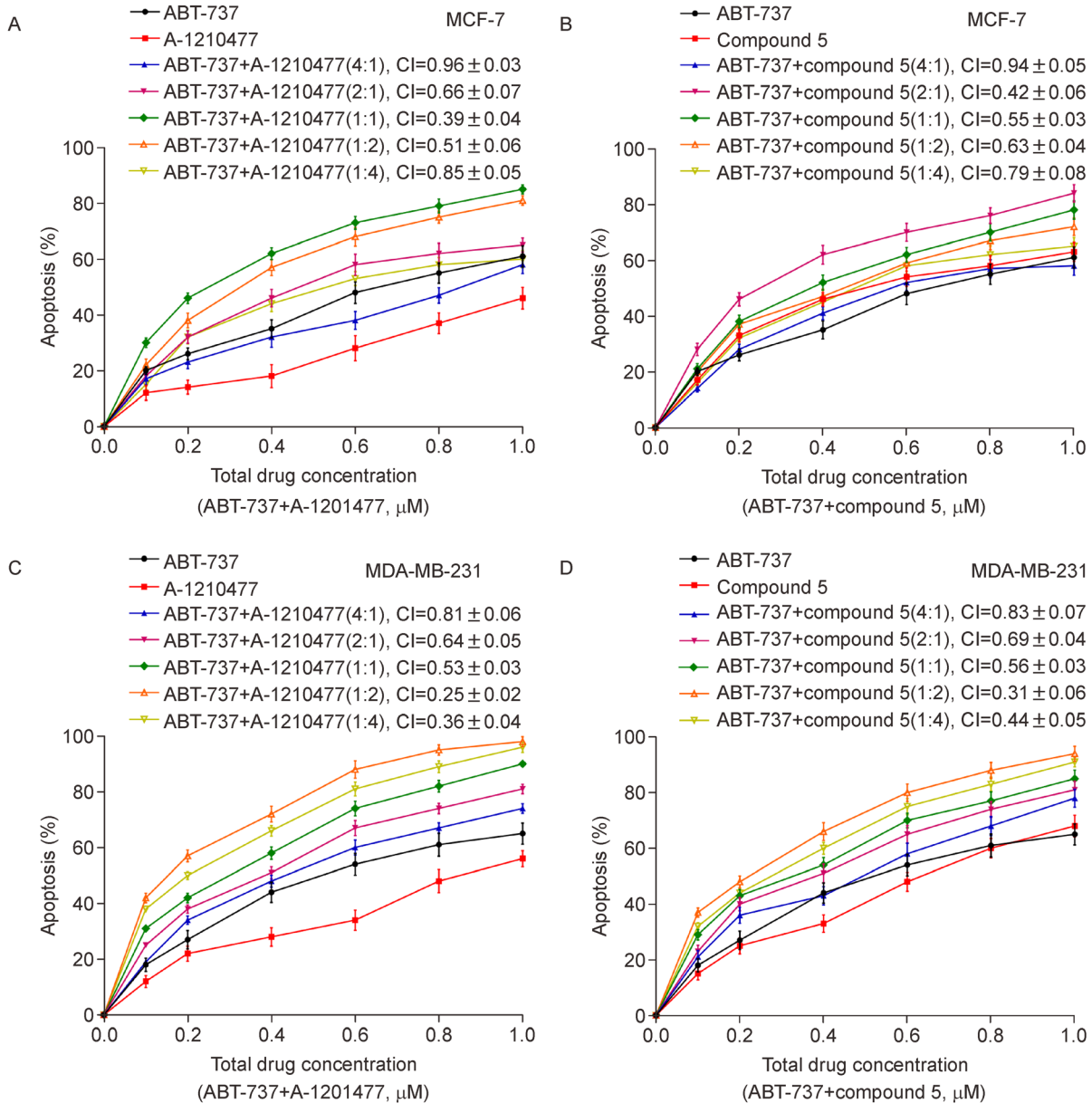

Figure 5. The best combination ratios of ABT-737/A-1210477 and ABT-737/compound 5 were experimentally verified in MCF-7 and MDA-MB-231. (A, B, C, D) MCF-7 and MDA-MB-231 cells were treated by compounds alone or in combination with fixed ratios for 48 h, after which the cell apoptosis assay determined the LC_{50}. The CI value was calculated by Calcusyn software using a methodology applied by Chou and Talalay. Data are the mean±stand deviation (sd) ($n = 3$).

significant roles determining Bcl-2 and/or Mcl-1 dependency.

A combined index of Bcl-2 and Mcl-1 better predicts the weights of Bcl-2 and Mcl-1

Next, we sought to obtain an equation comprising the protein levels of Bcl-2 and Mcl-1, which were termed [B] and [M], respectively, to predict the best drug ratio λ. By single-parameter sensitivity analysis, we determined that inhibitor-affected Mcl-1 degradation had a significant effect on the weights. Thus, we separately fitted the weights of Bcl-2 and Mcl-1 in the context of Mcl-1 inhibitors that decreased and increased Mcl-1 degradation as exemplified by ABT-737/A-1210477 and ABT-737/compound 5, respectively. By using the MATLAB curve fitting toolbox, we obtained multiple linear regression Eqs. (1) and (2) to predict the best drug ratio λ for a combination of Bcl-2 inhibitor with either of the Mcl-1 inhibitors that decrease and increase the Mcl-1 degradation rate, respectively. When comparing the prediction results between the equation and the model, a fit of R^2 of

0.85 ($P < 0.001$) and 0.71 ($P < 0.001$), respectively for ABT-737/A-1210477 (Eq. (1)) and ABT-737/compound 5 (Eq. (2)) was gained, indicating that the equations could well recapitulate the model prediction. When using the equations to predict the best drug ratio in MCF-7, MDA-MB-231, OCI-AML3, and HCT-116 cells, we obtained approximate λ values of 1, 0.5, 0.5, and 2 for ABT-737/A-1210477 and 2, 0.5, 1, and 2 for ABT-737/compound 5, respectively, which is in agreement with experimental data (Fig. 5 and Supplementary Fig. S1).

$$\text{ABT}-737/\text{A}-1210477:$$
$$(1)\begin{cases}\lambda=(0.35*[\text{B}]-128.22)/(128.22-[\text{M}]); & [\text{B}]/[\text{M}]>7.5\\ \lambda=(128.22-0.015*[\text{B}])/([\text{M}]-40.36); & [\text{B}]/[\text{M}]<2.5\\ \lambda=(48.92*[\text{B}]-20.24*[\text{M}])/(42.69*[\text{B}]-20.67*[\text{M}]); & 2.5<[\text{B}]/[\text{M}]<7.5\end{cases}$$

$$\text{ABT}-737/\text{compound 5}:$$
$$(2)\begin{cases}\lambda=(0.35*[\text{B}]-128.22)/(128.22-[\text{M}]); & [\text{B}]/[\text{M}]>7.5\\ \lambda=(87.86+0.45*[\text{B}])/([\text{M}]-40.36); & [\text{B}]/[\text{M}]<2.5\\ \lambda=(48.92*[\text{B}]-20.24*[\text{M}])/(42.69*[\text{B}]-20.67*[\text{M}]); & 2.5<[\text{B}]/[\text{M}]<7.5\end{cases}$$

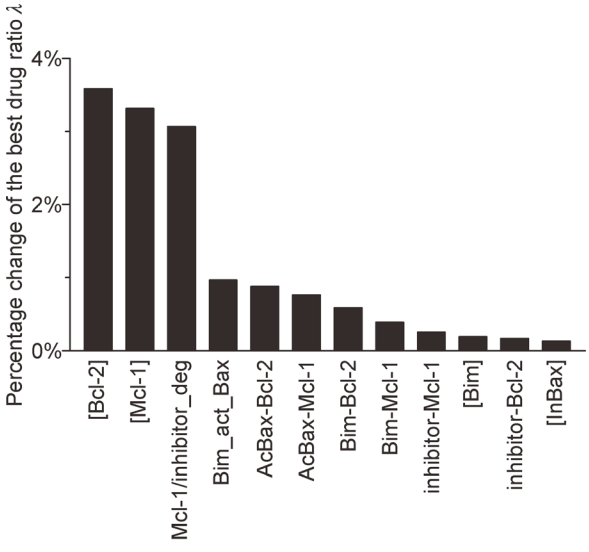

Figure 6. Percentage change of the best drug ratio λ in response to a 5% increase or decrease of each parameter. The first three bars indicate the most sensitive parameters which are protein levels of Bcl-2, Mcl-1, and Mcl-1/inhibitors degradation rate.

DISCUSSION

Cancer cells protect themselves from intrinsic mitochondrial apoptosis by upregulating anti-apoptotic members of the Bcl-2 protein family [4,5]. Pharmacological inhibition of anti-apoptotic Bcl-2 proteins can restore apoptosis and provide a useful therapeutic approach. The species of anti-apoptotic Bcl-2 family members and their expression levels differ greatly for individual cancer cells and have significant implications on choosing specific Bcl-2 inhibitors, Mcl-1 inhibitors, or their combination [38,39]. Many efforts have been made to study the molecular features of how cancer cells drive the dependencies of Bcl-2, Mcl-1, or their combinations and to find biomarkers or an index to predict the dependency [30,35,39,40]. It has been reported that Bcl-2 dependency is correlated with the expression level of Bcl-2 and could serve as a biomarker to predict treatment benefits from Bcl-2 inhibitors [14,39]. By correlation-relationship analysis and parameter sensitivity analysis, we determined that independent of Mcl-1 static level, the Mcl-1 production/degradation rate is a factor for Mcl-1 dependency. A similar study highlighted that no individual members of the Bcl-2 family proteins could predict responses to Mcl-1 inhibitors [40]. Our study demonstrates that a mathematical model can be successfully used to predict cell responses to specific Bcl-2 and Mcl-1 inhibitors alone or in combination.

Our model is the first study to quantitatively explore the contribution of anti-apoptotic Bcl-2 proteins to apoptosis by the weights of Bcl-2 and Mcl-1. Judging from the mathematical model and its implementation, it is clear that Bcl-2 and Mcl-1 are major determinants for treatment susceptibility. Our model found, for the first time, that the concentration of Mcl-1 is determined by cell context and small molecules. For example, A-1210377 led to a decrease in the Mcl-1 degradation rate, while compound 5 induced increased the Mcl-1 degradation rate. As such, the Mcl-1 protein exhibits different impacts on the prevention of apoptosis when cells are exposed to the two compounds. Only by our model can this be rationally and quantitatively addressed.

Unlike compound 5, which promotes the QRN helical conformational switch leading Mule-dependent Mcl-1 ubiquitination [32], proteolysis-targeting chimera molecules (PROTACs), a class of heterobifunctional molecules, are new inhibitors to degrade Mcl-1 via the

ubiquitin-proteasome system [41,42]. It has been reported that PROTACs show better pharmacodynamics and overcome resistance better than small-molecule Mcl-1 inhibitors [43,44]. However, the complete deletion of Mcl-1 causes lethal cardiac failure and mitochondrial dysfunction [45]. Therefore, Bcl-2 and Mcl-1 need to be inhibited in a coordinated and balanced ratio to gain the best therapeutic effect. Our model can be used as an efficient tool to predict the best combination ratio of Bcl-2 inhibitors and Mcl-1 PROTACs by incorporating the Mcl-1 degradation rate of the PROTAC molecule as parameters.

The “bright point” and advantage of our model approach is to predict the best ratio for a combination strategy of Bcl-2 inhibitors before real experiments or treatment. For cancer cells, we have provided a time-saving tool to obtain Bcl-2 family protein levels as parameters in the model from the CCLE database as we described in the methods. Furthermore, it is generally difficult to obtain enough primary cells to screen for the best combination ratio from clinical samples. However, our model could be a good tool to guide treatment with protein array (chip) data to provide background Bcl-2 family protein level information.

A further layer of complexity in the regulation of MOMP sensitivity was added by a recent report where Bcl-xL promotes the retrotranslocation of Bax from the mitochondria into the cytosol, thereby limiting Bax cytotoxicity [26]. A mathematical model incorporating the Bax retranslocation by Bcl-xL demonstrated that it could predict MOMP in response to the BH3-only protein activator or sensitizer more accurately than without considering the mechanism. Considering this layer of regulation, our simplified model might be less accurate in predicting inhibitor doses correlated to treatment response across cell lines as in the above model. We focused on the weights of Bcl-2/Bcl-xL and Mcl-1 in the study, and the simplification might not influence the concentrations since the retrotranslocation activity is exhibited by Bcl-xL which is similar to Bcl-2 and Mcl-1 degradation rates [26].

Finally, we provided two sets of equations as time-saving tools to predict the best drug combination ratio for treatment.

MATERIALS AND METHODS

Cell culture and reagents

MCF-7, MDA-MB-231, OCI-AML3, and HCT-116 were obtained from the American Type Culture Collection (ATCC). STR profiling validated the identity of the cell lines before furnishing them to the research lab. To avoid contamination, all the cell lines were used within 6 months. The cultured cells were preserved in DMEM-high glucose or RPMI-1640 medium containing 10% FBS and penicillin/streptomycin at 37°C in 5% CO_2. Compound 5 was synthesized, as previously described [32]. ABT-737 and A-1210477 were purchased from APExBIO (A8193 and B6011, Beijing, China). Antibodies specific for Mcl-1 and Actin were purchased from Santa Cruz Biotechnology (sc-12756 and sc-8432, CA, USA).

Immunoblotting

MCF-7 cells were lysed in RIPA buffer (Solarbio, Beijing, China) containing Halt protease inhibitor cocktail (Pierce Biotechnology, Rockford, USA) for 30 minutes on ice and centrifuged at 12,000×*g* for 15 minutes at 4°C. The protein concentration of the supernatant was determined by BCA assay (Beyotime, Shanghai, China), and 100 μg of total protein was resolved in 12% SDS–PAGE. Proteins were then transferred to PVDF membranes using the Bio-Rad system, blocked for 60 minutes in phosphate buffered saline with 0.1% Tween (PBST) containing 5% skim milk (BD Biosciences, USA), and incubated with primary antibody overnight in PBST at 4°C followed by incubating with HRP-conjugated secondary antibody for 60 minutes at room temperature. Blots were visualized with the use of a Super Signal West Pico Chemiluminescent Substrate (Pierce Biotechnology) and detected on a Kodak Image Station 4000MM Pro (New Haven, CT, USA).

Computational modeling

Protein-protein interactions, protein-small molecule inhibitors interactions, protein production and degradation, and protein activation were modeled using mass-action kinetics. Then, we transferred these formulations into a set of ordinary differential equations (ODEs) (Supplementary Table S1). MATLAB’s (The MathWorks Inc., Natick, MA, US) (RRID: SCR_001622) function *ode 15sec* was applied to solve the formulations. ODEs for Bcl-2 protein interaction and concentration of Bcl-2, Mcl-1, Bax, Bak, Bim, and Puma were parameterized according to literature reports or our previous experiments (Supplementary Tables S2–S6). The value of k_{pro} /k_{deg} was used to model for Proteins’ turnover to achieve equilibrium concentrations. The degradation rate of Mcl-1/A-1210477 and Mcl-1/compound 5 complex respectively were fitted by experimental data (Supplementary Table S4) with the MATLAB Optimization Toolbox. After that, we used MATLAB to solve the ODEs at time point t = 300 min.

To model the synergistic effect of ABT-737/A-1210477 or ABT-737/compound 5, we used a single dose or combined dose of the compounds as model inputs, and the output was the minimal dose that triggered MOMP.

Then, the combination index (CI) was calculated by Calcusyn software, which utilizes the Chou-Talalay method.

Obtainable prior model information and hypothesis involving network

An uncomplicated apoptotic network was constructed and centered around the regulation of the mitochondrial outer-membrane permeabilization (MOMP). MOMP leads to non-reversible cell death by releasing apoptotic factors such as cytochrome c and Smac/DIABLO from the mitochondria to the cytosol. The translocating channel MAC (Mitochondrial Apoptosis-induced Channel) was structured with Bax/Bak. The phenomenon of mitochondrial depolarization is regulated through interactions among the Bcl-2 family proteins. The Bcl-2 family proteins have classically been grouped into either pro- or anti-apoptotic members by function and sequence homology. Pro-apoptotic members include multi-domain effectors (BAX and BAK), the BH3-only proteins, referred to as "activators" (Bim and Puma), and the anti-apoptotic members include Bcl-2, Bcl-xL, and Mcl-1, they sequester pro-apoptotic members to inhibit MOMP.

Cell apoptosis assay

Cultured cells were seeded onto 6-well plates and treated with a gradient concentration of ABT-737, A-1210477, and compound 5 alone or in combination for 48 h. An Annexin V-FITC Apoptosis Detection Kit (Nanjing KeyGen BioTech Co., Ltd., Nanjing, China) was used to detect apoptosis using flow cytometry. According to the manufacturer's instructions, cells were washed twice with phosphate buffered saline (PBS) and incubated in a 1:40 solution of FITC-con-jugated Annexin V in the dark for 10 min at room temperature. The Annexin V-FITC positive cells were analyzed by flow cytometry on a BD FACSCalibur (BD Biosciences). CellQuest software (BD Biosciences) was used to determine the percentage of apoptosis in the samples. The lethal concentration 50 (LC_{50}) was defined as the concentration of small-molecule inhibitors to kill 50% of cells.

Combination index (CI) values analysis

Fraction of cells affected (Fa = 0.5) by different treatments were used to produce dose-response curves for ABT-737, A-1210477 and compound 5 alone or in combination. The CI value was calculated and the combination effect was assessed by Calcusyn software (Biosoft, Ferguson, MO, USA). A CI value less than, equal to, or greater than 1.0 indicated synergy, additivity, or antagonism for drug interactions.

Determination of intracellular protein concentration

The absolute intracellular protein concentrations of Bcl-2, Bcl-xL, Mcl-1, Bim, Puma, Bax, and Bak in MDA-MB-231, MCF-7, OCI-AML3, and HCT-116 were determined in our published report [46,47]. For other cell lines, the Cancer Cell Line Encyclopedia (CCLE) database was used to obtain quantitation data. First, all of the protein and mRNA expression levels can be downloaded from CCLE datasets, which are available on the CCLE portal (www.broadinstitute.org/ccle) and DepMap portal (www.depmap.org). In CCLE datasets, the relative protein levels are determined by "Reverse Phase Protein Array (RPPA)," and the relative mRNA expression levels are evaluated in "Affymetrix U133 Plus 2.0 arrays," both of which are $\log_2$-transformed RMA-normalized data. Furthermore, the median translation rates across all tissues addressed by Wihelm *et al*. were used to convert the transcript amounts to protein abundance [48]. Second, the absolute intracellular protein concentrations of Bcl-2, Bcl-xL, Mcl-1, Bim, Puma, Bax, and Bak in MCF-7 served as a reference. The protein levels in other cell lines were directly normalized to levels in MCF-7 cells, so each protein concentration was proportional to the corresponding one in the MCF-7 cells.

Statistical analysis

Results were expressed as mean ± standard deviation (s.d.) of three independent experiments. The levels of significance were assessed by a two-tailed *t*-test using GraphPad, Prism 6.0 software (GraphPad Software, Inc., La Jolla, CA, USA). $P < 0.05$ was considered significant. A correlation analysis was performed to determine the prediction results between the equations and model. The grade of liner dependency was evaluated by Pearson's correlation coefficient. For analysis, the MATLAB function *corr* was used. A correlation coefficient close to or equal to one was assumed to signify a good correlation.

SUPPLEMENTARY MATERIALS

The supplementary materials can be found online with this article at https://doi.org/10.15302/J-QB-021-0237.

ACKNOWLEDGEMENTS

This research was supported by the National Natural Science Foundation of China (81430083, 81903462 and 82073703), the China Postdoctoral Science Foundation (2018M641694), and the Fundamental Research Funds for the Central Universities (DUT20LK28 and DUT20YG133).

COMPLIANCE WITH ETHICS GUIDELINES

The authors Zongwei Guo, Fangkui Yin, Peiran Wang, Ting Song and Zhichao Zhang declare that they have no conflict of interests.

This article does not contain any studies with human or animal subjects performed by any of the authors.

OPEN ACCESS

REFERENCES

1. Leber, B., Lin, J. and Andrews, D. W. (2007) Embedded together: the life and death consequences of interaction of the Bcl-2 family with membranes. Apoptosis, 12, 897–911
2. van Delft, M. F. and Huang, D. C. (2006) How the Bcl-2 family of proteins interact to regulate apoptosis. Cell Res., 16, 203–213
3. García-Sáez, A. J. (2012) The secrets of the Bcl-2 family. Cell Death Differ., 19, 1733–1740
4. Certo, M., Del Gaizo Moore, V., Nishino, M., Wei, G., Korsmeyer, S., Armstrong, S. A. and Letai, A. (2006) Mitochondria primed by death signals determine cellular addiction to antiapoptotic BCL-2 family members. Cancer Cell, 9, 351–365
5. Opferman, J. T. (2016) Attacking cancer’s Achilles heel: antagonism of anti-apoptotic BCL-2 family members. FEBS J., 283, 2661–2675
6. Dewson, G. and Kluck, R. M. (2009) Mechanisms by which Bak and Bax permeabilise mitochondria during apoptosis. J. Cell Sci., 122, 2801–2808
7. Shamas-Din, A., Kale, J., Leber, B. and Andrews, D. W. (2013) Mechanisms of action of Bcl-2 family proteins. Cold Spring Harb. Perspect. Biol., 5, a008714
8. Lee, S., Park, K. and Kim, D. (2009) Building a drug-target network and its applications. Expert Opin. Drug Discov., 4, 1177–1189
9. Adams, J. M. and Cory, S. (2007) The Bcl-2 apoptotic switch in cancer development and therapy. Oncogene, 26, 1324–1337
10. Youle, R. J. and Strasser, A. (2008) The BCL-2 protein family: opposing activities that mediate cell death. Nat. Rev. Mol. Cell Biol., 9, 47–59
11. Chipuk, J. E., Moldoveanu, T., Llambi, F., Parsons, M. J. and Green, D. R. (2010) The BCL-2 family reunion. Mol. Cell, 37, 299–310
12. Chen, L., Willis, S. N., Wei, A., Smith, B. J., Fletcher, J. I., Hinds, M. G., Colman, P. M., Day, C. L., Adams, J. M. and Huang, D. C. (2005) Differential targeting of prosurvival Bcl-2 proteins by their BH3-only ligands allows complementary apoptotic function. Mol. Cell, 17, 393–403
13. Oltersdorf, T., Elmore, S. W., Shoemaker, A. R., Armstrong, R. C., Augeri, D. J., Belli, B. A., Bruncko, M., Deckwerth, T. L., Dinges, J., Hajduk, P. J., *et al.* (2005) An inhibitor of Bcl-2 family proteins induces regression of solid tumours. Nature, 435, 677–681
14. Del Gaizo Moore, V., Brown, J. R., Certo, M., Love, T. M., Novina, C. D. and Letai, A. (2007) Chronic lymphocytic leukemia requires BCL2 to sequester prodeath BIM, explaining sensitivity to BCL2 antagonist ABT-737. J. Clin. Invest., 117, 112–121
15. Tahir, S. K., Yang, X., Anderson, M. G., Morgan-Lappe, S. E., Sarthy, A. V., Chen, J., Warner, R. B., Ng, S. C., Fesik, S. W., Elmore, S. W., *et al.* (2007) Influence of Bcl-2 family members on the cellular response of small-cell lung cancer cell lines to ABT-737. Cancer Res., 67, 1176–1183
16. Vogler, M., Dinsdale, D., Sun, X. M., Young, K. W., Butterworth, M., Nicotera, P., Dyer, M. J. and Cohen, G. M. (2008) A novel paradigm for rapid ABT-737-induced apoptosis involving outer mitochondrial membrane rupture in primary leukemia and lymphoma cells. Cell Death Differ., 15, 820–830
17. van Delft, M. F., Wei, A. H., Mason, K. D., Vandenberg, C. J., Chen, L., Czabotar, P. E., Willis, S. N., Scott, C. L., Day, C. L., Cory, S., *et al.* (2006) The BH3 mimetic ABT-737 targets selective Bcl-2 proteins and efficiently induces apoptosis via Bak/Bax if Mcl-1 is neutralized. Cancer Cell, 10, 389–399
18. Nguyen, M., Marcellus, R. C., Roulston, A., Watson, M., Serfass, L., Murthy Madiraju, S. R., Goulet, D., Viallet, J., Bélec, L., Billot, X., *et al.* (2007) Small molecule obatoclax (GX15-070) antagonizes MCL-1 and overcomes MCL-1-mediated resistance to apoptosis. Proc. Natl. Acad. Sci. USA, 104, 19512–19517
19. Li, Z., He, S. and Look, A. T. (2019) The MCL1-specific inhibitor S63845 acts synergistically with venetoclax/ABT-199 to induce apoptosis in T-cell acute lymphoblastic leukemia cells. Leukemia, 33, 262–266
20. Moujalled, D. M., Pomilio, G., Ghiurau, C., Ivey, A., Salmon, J., Rijal, S., Macraild, S., Zhang, L., Teh, T. C., Tiong, I. S., *et al.* (2019) Combining BH3-mimetics to target both BCL-2 and MCL1 has potent activity in pre-clinical models of acute myeloid leukemia. Leukemia, 33, 905–917
21. Lee, E. F., Harris, T. J., Tran, S., Evangelista, M., Arulananda, S., John, T., Ramnac, C., Hobbs, C., Zhu, H., Gunasingh, G., *et al.* (2019) BCL-XL and MCL-1 are the key BCL-2 family proteins in melanoma cell survival. Cell Death Dis., 10, 342
22. Algarín, E. M., Díaz-Tejedor, A., Mogollón, P., Hernández-García, S., Corchete, L. A., San-Segundo, L., Martín-Sánchez, M., González-Méndez, L., Schoumacher, M., Banquet, S., *et al.* (2020) Preclinical evaluation of the simultaneous inhibition of MCL-1 and BCL-2 with the combination of S63845 and venetoclax in multiple myeloma. Haematologica, 105, e116–e120
23. Lindner, A. U., Concannon, C. G., Boukes, G. J., Cannon, M. D., Llambi, F., Ryan, D., Boland, K., Kehoe, J., McNamara, D. A., Murray, F., *et al.* (2013) Systems analysis of BCL2 protein family

interactions establishes a model to predict responses to chemotherapy. Cancer Res., 73, 519–528
24. Lindner, A. U., Salvucci, M., Morgan, C., Monsefi, N., Resler, A. J., Cremona, M., Curry, S., Toomey, S., O'Byrne, R., Bacon, O., *et al.* (2017) BCL-2 system analysis identifies high-risk colorectal cancer patients. Gut, 66, 2141–2148
25. Lucantoni, F., Lindner, A. U., O'Donovan, N., Düssmann, H. and Prehn, J. H. M. (2018) Systems modeling accurately predicts responses to genotoxic agents and their synergism with BCL-2 inhibitors in triple negative breast cancer cells. Cell Death Dis., 9, 42
26. Hantusch, A., Das, K. K., García-Sáez, A. J., Brunner, T. and Rehm, M. (2018) Bax retrotranslocation potentiates Bcl-x_L's antiapoptotic activity and is essential for switch-like transitions between MOMP competency and resistance. Cell Death Dis., 9, 430
27. Czabotar, P. E., Lee, E. F., van Delft, M. F., Day, C. L., Smith, B. J., Huang, D. C. S., Fairlie, W. D., Hinds, M. G. and Colman, P. M. (2007) Structural insights into the degradation of Mcl-1 induced by BH3 domains. Proc. Natl. Acad. Sci. USA, 104, 6217–6222
28. Yang, T., Buchan, H. L., Townsend, K. J. and Craig, R. W. (1996) MCL-1, a member of the BLC-2 family, is induced rapidly in response to signals for cell differentiation or death, but not to signals for cell proliferation. J. Cell. Physiol., 166, 523–536
29. Nijhawan, D., Fang, M., Traer, E., Zhong, Q., Gao, W., Du, F. and Wang, X. (2003) Elimination of Mcl-1 is required for the initiation of apoptosis following ultraviolet irradiation. Genes Dev., 17, 1475–1486
30. Zhang, H., Guttikonda, S., Roberts, L., Uziel, T., Semizarov, D., Elmore, S. W., Leverson, J. D. and Lam, L. T. (2011) Mcl-1 is critical for survival in a subgroup of non-small-cell lung cancer cell lines. Oncogene, 30, 1963–1968
31. Leverson, J. D., Zhang, H., Chen, J., Tahir, S. K., Phillips, D. C., Xue, J., Nimmer, P., Jin, S., Smith, M., Xiao, Y., *et al.* (2015) Potent and selective small-molecule MCL-1 inhibitors demonstrate on-target cancer cell killing activity as single agents and in combination with ABT-263 (navitoclax). Cell Death Dis., 6, e1590
32. Song, T., Wang, Z., Ji, F., Feng, Y., Fan, Y., Chai, G., Li, X., Li, Z. and Zhang, Z. (2016) Deactivation of Mcl-1 by dual-function small-molecule inhibitors targeting the Bcl-2 homology 3 domain and facilitating Mcl-1 ubiquitination. Angew. Chem. Int. Ed. Engl., 55, 14250–14256
33. Tokar, T. and Ulicny, J. (2013) The mathematical model of the Bcl-2 family mediated MOMP regulation can perform a non-trivial pattern recognition. PLoS One, 8, e81861
34. Adams, J. M. and Cory, S. (2007) The Bcl-2 apoptotic switch in cancer development and therapy. Oncogene, 26, 1324–1337
35. Soderquist, R. S., Crawford, L., Liu, E., Lu, M., Agarwal, A., Anderson, G. R., Lin, K. H., Winter, P. S., Cakir, M. and Wood, K. C. (2018) Systematic mapping of BCL-2 gene dependencies in cancer reveals molecular determinants of BH3 mimetic sensitivity. Nat. Commun., 9, 3513
36. Song, T., Zhang, M., Liu, P., Xue, Z., Fan, Y. and Zhang, Z. (2018) Identification of JNK1 as a predicting biomarker for ABT-199 and paclitaxel combination treatment. Biochem. Pharmacol., 155, 102–109
37. Song, T., Chai, G., Liu, Y., Yu, X., Wang, Z. and Zhang, Z. (2016) Bcl-2 phosphorylation confers resistance on chronic lymphocytic leukaemia cells to the BH3 mimetics ABT-737, ABT-263 and ABT-199 by impeding direct binding. Br. J. Pharmacol., 173, 471–483
38. Touzeau, C., Ryan, J., Guerriero, J., Moreau, P., Chonghaile, T. N., Le Gouill, S., Richardson, P., Anderson, K., Amiot, M. and Letai, A. (2016) BH3 profiling identifies heterogeneous dependency on Bcl-2 family members in multiple myeloma and predicts sensitivity to BH3 mimetics. Leukemia, 30, 761–764
39. Al-Harbi, S., Hill, B. T., Mazumder, S., Singh, K., Devecchio, J., Choudhary, G., Rybicki, L. A., Kalaycio, M., Maciejewski, J. P., Houghton, J. A., *et al.* (2011) An antiapoptotic BCL-2 family expression index predicts the response of chronic lymphocytic leukemia to ABT-737. Blood, 118, 3579–3590
40. Goodwin, C. M., Rossanese, O. W., Olejniczak, E. T. and Fesik, S. W. (2015) Myeloid cell leukemia-1 is an important apoptotic survival factor in triple-negative breast cancer. Cell Death Differ., 22, 2098–2106
41. Wang, Z., He, N., Guo, Z., Niu, C., Song, T., Guo, Y., Cao, K., Wang, A., Zhu, J., Zhang, X., *et al.* (2019) Proteolysis targeting chimeras for the selective degradation of Mcl-1/Bcl-2 derived from nonselective target binding ligands. J. Med. Chem., 62, 8152–8163
42. Lebraud, H. and Heightman, T. D. (2017) Protein degradation: a validated therapeutic strategy with exciting prospects. Essays Biochem., 61, 517–527
43. Papatzimas, J. W., Gorobets, E., Maity, R., Muniyat, M. I., MacCallum, J. L., Neri, P., Bahlis, N. J. and Derksen, D. J. (2019) From inhibition to degradation: targeting the antiapoptotic protein myeloid cell leukemia 1 (MCL1). J. Med. Chem., 62, 5522–5540
44. An, S. and Fu, L. (2018) Small-molecule PROTACs: An emerging and promising approach for the development of targeted therapy drugs. EBioMedicine, 36, 553–562
45. Wang, X., Bathina, M., Lynch, J., Koss, B., Calabrese, C., Frase, S., Schuetz, J. D., Rehg, J. E. and Opferman, J. T. (2013) Deletion of MCL-1 causes lethal cardiac failure and mitochondrial dysfunction. Genes Dev., 27, 1351–1364
46. Song, T., Wang, P., Yu, X., Wang, A., Chai, G., Fan, Y. and Zhang, Z. (2019) Systems analysis of phosphorylation-regulated Bcl-2 interactions establishes a model to reconcile the controversy over the significance of Bcl-2 phosphorylation. Br. J. Pharmacol., 176, 491–504
47. Guo, Z., Song, T., Xue, Z., Liu, P., Zhang, M., Zhang, X. and Zhang, Z. (2020) Using CETSA assay and a mathematical model to reveal dual Bcl-2/Mcl-1 inhibition and on-target mechanism for ABT-199 and S1. Eur. J. Pharm. Sci., 142, 105105
48. Wilhelm, M., Schlegl, J., Hahne, H., Gholami, A. M., Lieberenz, M., Savitski, M. M., Ziegler, E., Butzmann, L., Gessulat, S., Marx, H., *et al.* (2014) Mass-spectrometry-based draft of the human proteome. Nature, 509, 582–587